

Structure and Mechanism of the Caseinolytic Protease ClpP1/2 Heterocomplex from *Listeria monocytogenes***

Maria Dahmen, Marie-Theres Vielberg, Michael Groll,* and Stephan A. Sieber*

Abstract: *Listeria monocytogenes* is a devastating bacterial pathogen. Its virulence and intracellular stress tolerance are supported by caseinolytic protease P (ClpP), an enzyme that is conserved among bacteria. *L. monocytogenes* expresses two ClpP isoforms that are only distantly related by sequence and differ in catalysis, oligomerization, active-site composition, and N-terminal interaction sites for associated AAA⁺ chaperones. The crystal structure of the ClpP1/2 heterocomplex from *L. monocytogenes* was solved, and in combination with biochemical studies, it provides insights into the mode of action. The results demonstrate that structural interlocking of LmClpP1 with LmClpP2 leads to the formation of a tetradecamer, aligns all 14 active sites, and enhances proteolytic activity. Furthermore, the catalytic center was identified as being responsible for the transient stability of ClpPs.

In prokaryotic organisms, protein digestion is carried out by a variety of ATP-dependent proteases. One member with essential regulatory roles for the DNA-damage response, cell homeostasis, and virulence is the caseinolytic protease P (ClpP).^[1] It assembles into a barrel-shaped tetradecameric complex consisting of two heptameric rings that are stacked face-to-face.^[2] Although ClpP can cleave small peptides, the axial pores restrict the degradation of larger protein chains.^[3] For controlled proteolysis, the apical sites of the cylinder associate with AAA⁺ chaperones (e.g. ClpX, ClpA, and ClpC) that recognize, unfold, and direct larger protein substrates into the proteolytic chamber in an ATP-dependent process.^[4] ClpXP is ubiquitously required to remove damaged and SsrA-tagged proteins stalled at the ribosome under

cellular stress conditions.^[5] Several reports demonstrate an additional role for ClpXP in virulence regulation of pathogenic bacteria such as *Listeria monocytogenes*.^[1c,6] In contrast to the majority of bacterial organisms, *L. monocytogenes* and *Mycobacterium tuberculosis* encode two ClpP isoforms.^[7] Little is known about the role of these isoforms and subtle differences between species are observed. In *L. monocytogenes*, a food-borne pathogen that invades and multiplies within host cells,^[8] LmClpP2 is essential for virulence while the function of LmClpP1 is unknown.^[6] LmClpP2 forms an active tetradecameric enzyme that shares 66 % sequence identity with ClpP from *Escherichia coli*.^[7a,9] LmClpP1 exhibits 44 % sequence identity, but is truncated at the N terminus. Besides, the active-site residue Asp is exchanged for an Asn, thus leading to a major alteration in the catalytic triad (Figure S1 in the Supporting Information). It is expressed as an inactive heptamer, which only gains peptidolytic activity when associated in a tetradecameric heterocomplex with LmClpP2.^[9] Recently, homooligomeric crystal structures of LmClpP1 (PDB: 4JCQ) and LmClpP2 (PDB: 4JCT) in an inactive state with misaligned catalytic centers (Ser98, His123, Asp/Asn172; numbering according to Figure S1^[9]) were obtained, thus raising questions regarding the functional interaction of the two enzymes. Herein, we present structural and biochemical data for the active LmClpP1/2 heterocomplex that reveal 14 aligned active sites, enhanced proteolytic activity, and a unidirectional interaction with the associated LmClpX chaperone.


A major limitation in previous preparations of the LmClpP1/2 heterocomplex was the varying ratio of ClpP1/ClpP2.^[7a,9] We thus introduced a new co-expression system in which LmClpP1 possesses a C-terminal Strep-tag and LmClpP2 a C-terminal His-tag (Figure S2). Alternating Ni- and Strep-affinity chromatography of the co-expressed lysates led to the isolation of LmClpP1/2 in a 1:1 ratio after size-exclusion chromatography. These findings were confirmed by mass-spectrometry (Figure S3). Notably, adding 1 % CHAPS to the lysis buffer significantly increased the yield by up to 150-fold (Figure S4 and S5).

LmClpP1/2 was evaluated for peptidase activity with a previously established fluorescent tripeptide substrate (Leu-ACC)^[9] and found to exhibit a 40 % reduced rate of peptide hydrolysis compared to the LmClpP2 homocomplex (Figure 1 A). To study the individual enzyme activities within the heterocomplex, we introduced active-site mutations (Ser98Ala) in either LmClpP1 or LmClpP2. Although LmClpP1/2(S98A) exhibited enhanced peptidase activity compared to LmClpP1 alone, the rate was about 10-fold reduced compared to the LmClpP2 homocomplex and 5-fold reduced compared to LmClpP1(S98A)/2 (Figure 1 A). These

[*] M. Dahmen,^[‡] M.-T. Vielberg,^[‡] Prof. Dr. M. Groll, Prof. Dr. S. A. Sieber
Center for Integrated Protein Science Munich CIPS^M, Department of Chemistry, Technische Universität München
Lichtenbergstr. 4, 85747 Garching (Germany)
E-mail: michael.groll@tum.de
stephan.sieber@tum.de

[‡] These authors contributed equally to this work.

[**] We thank Mona Wolff and Katja Bäuml for excellent scientific support, Evelyn Zeiler and Malte Gersch for scientific discussions, and the staff of the beamline X06SA at the Paul Scherrer Institute, Swiss Light Source (Villingen, Switzerland) for help with data collection. Marcin Drag and Marcin Poreba are acknowledged for providing the tripeptide substrate. The work was funded by the Deutsche Forschungsgemeinschaft, SFB749, SFB1035, FOR1406 and the ERC starting grant (250924-antibacterials).

 Supporting information for this article (including details on cloning, protein purification, bioassays, crystallization, and structure analysis) is available on the WWW under <http://dx.doi.org/10.1002/anie.201409325>.

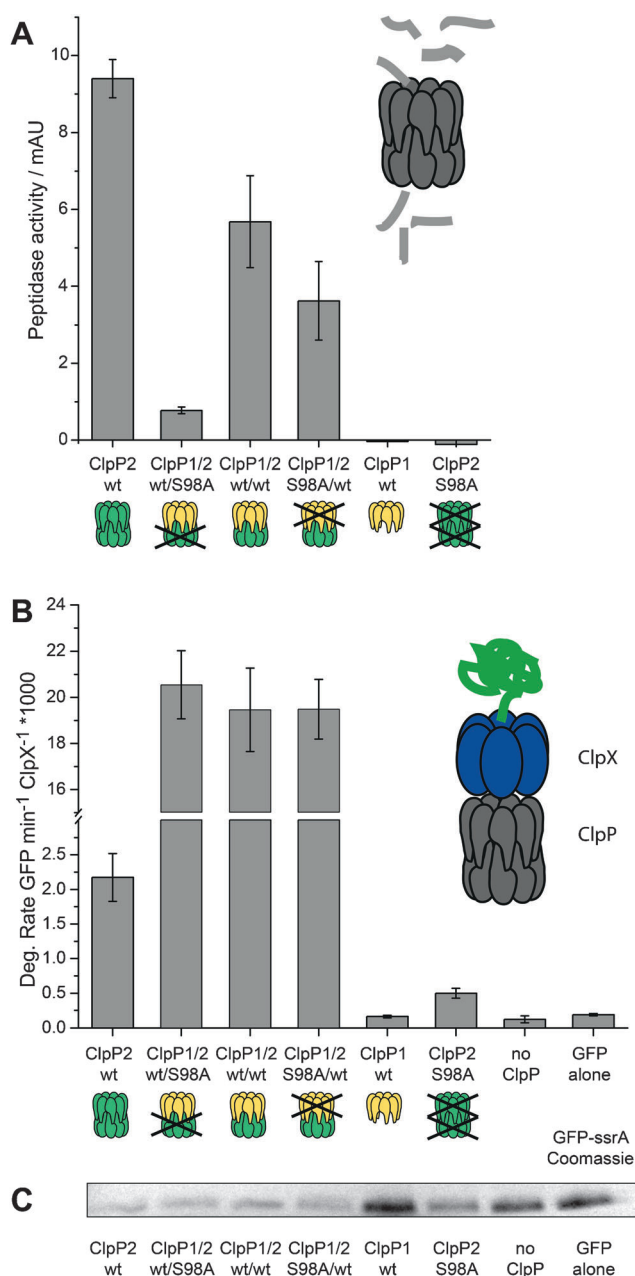


Figure 1. Heterocomplex activity. A) Peptidase activity of LmClpP proteins (1 μ M) measured with 100 μ M Leu-ACC at 37°C. B) Protease activity of LmClpP proteins (0.2 μ M LmClpP₁₄) in the presence of 0.4 μ M LmClpX₆ and 0.4 μ M GFP-SsrA in regeneration buffer. Both data sets represent three independent experiments (mean \pm standard deviation). C) Corresponding coomassie-stained gel of the GFP-SsrA digest after 3 h.

data suggest that even though LmClpP1 is significantly activated within the heterocomplex, its peptidolytic efficiency still lags behind LmClpP2. As expected, the hydrolytic activity of LmClpP1(S98A)/2 was half that of LmClpP2, thus indicating that two active heptameric rings are required for maximal peptidase activity.

Next, we investigated the proteolytic properties of the ClpP complexes in association with LmClpX, an AAA⁺ chaperone in *L. monocytogenes*. LmClpX was cloned, over-

expressed, and purified in its ATPase-active state (Figure S6). To monitor the proteolytic rate of the LmClpXP1/2 complex, we constructed a green fluorescent protein (GFP) fused to a C-terminal SsrA-tag as reported previously.^[10] Since ATP-dependent chaperones in complex with ClpP can recognize and unfold GFP-SsrA without digestion,^[10] we first determined the background rate in a system in which LmClpX is mixed with inactivated LmClpP2(S98A) (Figure 1 B,C). Afterwards the proteolytic activity of LmClpP2 was investigated by incubating it with LmClpX. Digestion of GFP was observed by a decrease in fluorescence intensity and a vanishing band on SDS-PAGE (Figure 1 C). Surprisingly, an up to 9-fold increase in proteolytic activity was observed when LmClpP1/2, LmClpP1(S98A)/2, and LmClpP1/2(S98A) were incubated with LmClpX. This rate enhancement was not a consequence of increased LmClpX activity since neither LmClpP2 nor the heterocomplex altered the rate of ATP hydrolysis (Figure S6). While LmClpP1 is catalytically impaired in peptide assays, it still retains sufficient activity to substitute for LmClpP2 in proteolysis. Interestingly, mycobacterial ClpP1/2 in association with the chaperone MtClpC1 also revealed elevated proteolytic rates when one of the two ClpP rings was inactivated, thus supporting our findings that, at least in heterocomplexes, the peptidolytic and proteolytic activities are decoupled.^[11]

In contrast to LmClpP2, one striking feature of LmClpP1 is its lower sequence identity with other ClpPs, especially with regards to the N terminus of the subunits. Severe deviations in conserved recognition sequences indicate that an association with AAA⁺ chaperones is impossible.^[12] This suggests that LmClpX binds to the heterocomplex solely through the LmClpP2 site. To investigate this hypothesis, we utilized a previously established constitutively activate LmClpP1-(N172D) mutant that forms a tetradecamer with peptidase activity (Figure S7).^[9] No proteolysis was observed upon the addition of LmClpX, thus demonstrating that the active complex is incapable of chaperone binding (Figure S8). Although there are currently no structural data available for any ClpXP complex at high resolution, our results point towards a unidirectional binding of LmClpX exclusively to the LmClpP2 pore.

To determine the molecular interactions that are responsible for heterocomplex activity, we crystallized LmClpP1/2 and solved the structure by molecular replacement at 2.8 Å resolution ($R_{\text{free}} = 21.7\%$, Table S2, PDB: 4RYF). The heterocomplex consists of one homo-LmClpP1 and one homo-LmClpP2 heptamer stacked face-to-face to form a tetradecameric barrel (Figure 2 and Figure S9). Despite a pronounced deviation on the sequence level between the two LmClpPs (42% identity), the heterocomplex reveals an unexpected degree of structural identity. The enzyme exhibits a cylindrical shape with a height of 100 Å and a diameter of 95 Å. Structural superposition of LmClpP1 and LmClpP2 monomers shows clashes between the distinct adjacent subunits, thus ruling out the formation of mixed heptameric rings (Figure S10). The two heptameric rings of LmClpP1/2 are seamlessly interlocked through their adjacent extended E-helices, a major secondary structural element of each subunit involved in tetradecamer formation.^[13] Connected to these E-

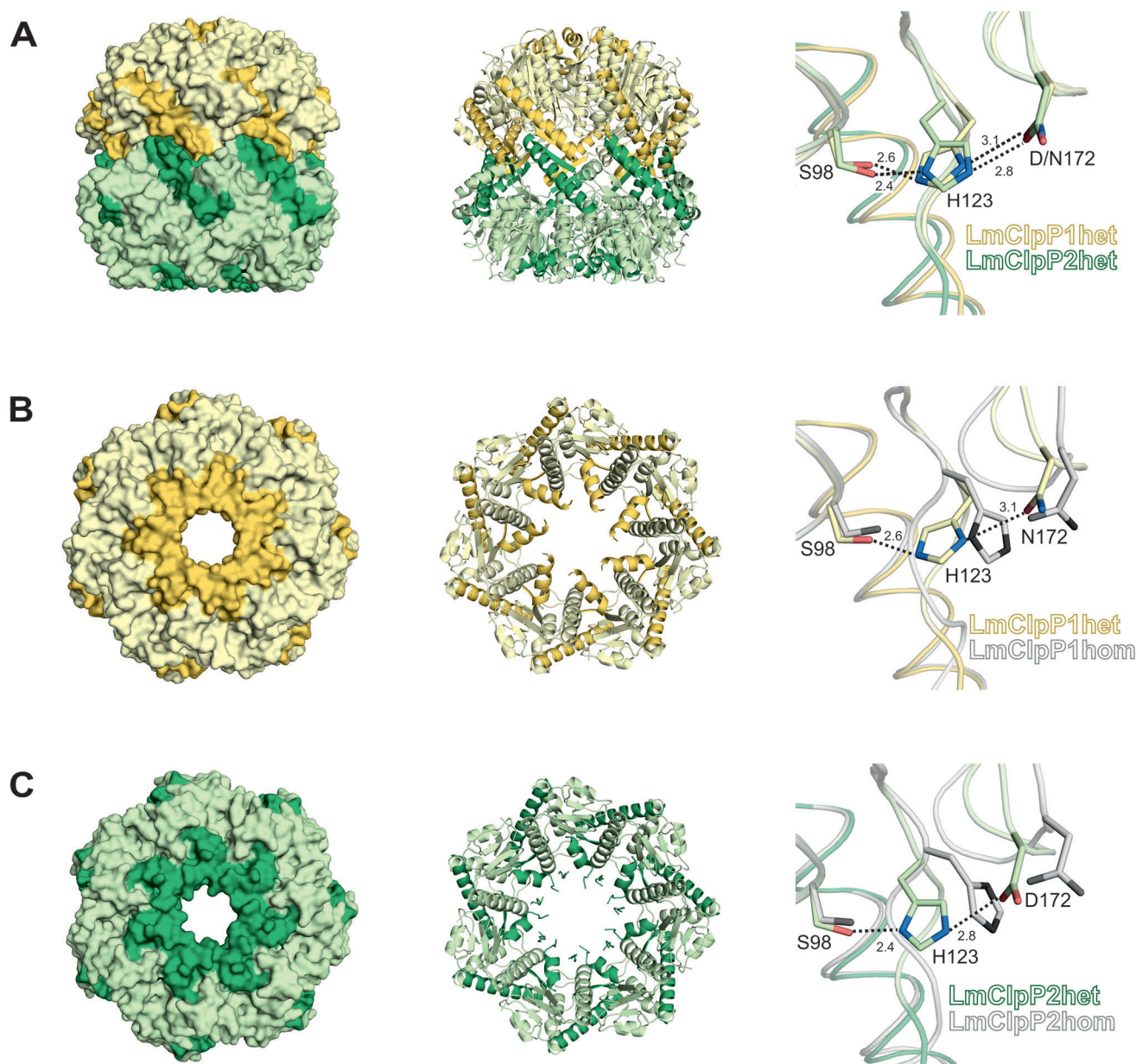


Figure 2. Crystal structure of the LmClpP1/2 heterocomplex (PDB Code: 4RYF). A) Side view of the heterocomplex of LmClpP1 (gold) and LmClpP2 (green) and an overlay of the aligned catalytic centers. B) Top view of the LmClpP1 interface of the heterocomplex and an overlay of the LmClpP1 catalytic residues Ser98, His123, and Asn172 in the homo- and heterocomplex. C) Top view of the LmClpP2 interface of the heterocomplex and an overlay of the LmClpP2 catalytic residues Ser98, His123, and Asp172 in the homo- and heterocomplex. Previously reported structures are shown in gray and the heteroatoms N and O in blue and red, respectively.

helices are β -sheet residues 126–131, which constitute an H-bond zipper for inter-ring stabilization (Figure S9B). Furthermore, a conserved Asp170–Arg171 sensor across the heptamer interface is aligned, and with its direct connection to the proteolytic center, this sensor represents an additional hallmark of ClpPs in an active state (Figure S9D).^[13,14] Major structural differences between LmClpP1 and LmClpP2 are observed at the apical sites of the heterocomplex. While the LmClpP2 units possess a rather flat docking site for LmClpX, LmClpP1 exhibits an unusual curved shape (Figure 2A) caused by N-terminal residues 17–28 (Figure S1), which form

a long helix that lines up the axial pore (Figure 2 and Figure 3A).

In contrast to the previously reported inactive structural arrangement in the LmClpP2 homocomplex, the catalytic triad is aligned in heterooligomeric LmClpP2 (Figure 2C). While isolated LmClpP1 displays a compressed conformation harboring a misaligned catalytic center, the association with LmClpP2 induces a catalytic Ser98–His123 dyad that is further stabilized by the polarization of Asn172 (Figure 2A,B). Accompanying this transition from the inactive to the active state, His123 and Asn172 perform large conformational rotations that not only coordinate the activation of Ser98

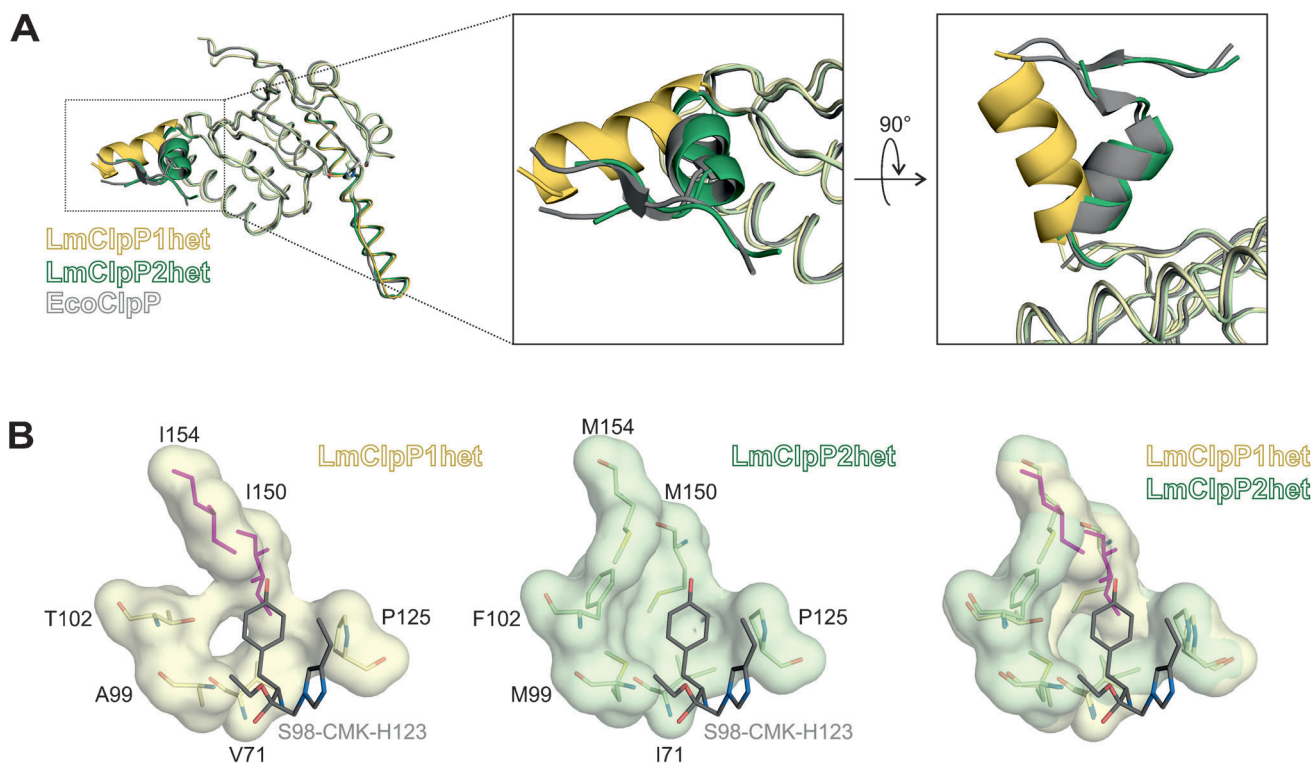


Figure 3. A) Overlay of heterooligomeric LmClpP1 and LmClpP2 with EcClpP. B) S1 pocket of heterooligomeric LmClpP1 and LmClpP2 with an overlay of the EcClpP active-site inhibitor Z-LY-CMK (colored in gray). Residues 150 and 154 of LmClpP1, which are responsible for reduction of the size of the S1 pocket and the steric clash with the Tyr residue, are shown in pink (remaining colors as in Figure 2).

but also extend the E-helix and align the Asp170-Arg171 sensor (Figure S9A,D). Interestingly, although the carbonyl oxygen atom of Asn172 can only interact with His123 through weak H bonds (compared to Asp172 in LmClpP2), its presence is crucial for acylation activity, as demonstrated by an inactive Asn172Ala mutation.^[7a] Moreover, the observed rotation of Asn172 to align with His123 in the active state points towards an essential mechanism that involves the action of all three catalytic residues.

Strikingly, the LmClpP1/2 structure revealed no additional stabilization compared to LmClpP2, only strict conservation of key interaction sites (Figure S9). The lower melting temperature of LmClpP1/2 versus LmClpP2, as observed in thermal shift assays, implies that LmClpP1/2 forms a transient heterocomplex that co-exists with LmClpP2 tetradecamers and LmClpP1 heptamers (Figure S11).

A structural overlay of *E. coli* ClpP bound to Z-LY-chloromethylketone (CMK, PDB: 2FZS)^[15] with the unliganded LmClpP1/2 heterocomplex enabled the assignment of the corresponding S1 substrate pockets (Figure 3B). While LmClpP2 and EcClpP exhibit a similar organization and size of their binding sites, which are lined by conserved residues, the available space within LmClpP1 is restricted by Ile150 and Ile154 (Figure 3B and Figure S12). This modification leads to a smaller and more defined specificity pocket, thus limiting the access of large residues such as P1-Tyr, which is in line with the previously observed preference of LmClpP1 for P1-Leu substrates for peptide cleavage.^[9] Similarly, β -lactone inhibitors with extended side chains only bound to LmClpP2,

while the ones with shorter residues also attached to LmClpP1.^[9] These results emphasize a specialization for different substrates and should facilitate the design of customized inhibitors that selectively address either LmClpP1 or LmClpP2.

In summary, the crystal structure of the *L. monocytogenes* ClpP1/2 heterocomplex provides insights into an unprecedented activation mechanism and a unidirectional interaction with ClpX that enables proteolysis at an enhanced rate, at least in *L. monocytogenes*. To form the heterocomplex, LmClpP2 and LmClpP1 mutually support each other to bind, pull, and extend its intrinsically disordered E-helix, thereby aligning all of the catalytic centers (Figure 2, Figure S13). Despite large deviations in the primary sequence, these key interactions are identical to the ones observed in homocomplexes and emphasize the high degree of structural conservation. The heterooligomeric LmClpP1/2 structure further reveals a general ClpP mechanism by which the catalytic residues Asn and Asp172 play a key role in complex stability, oligomerization, and activity. Previous ClpP structures crystallized at low pH values show a protonated Asp172, which thus mimics Asn172. Remarkably, all these structures are characterized by misalignment of the active site and adopt the inactive, compressed state. Moreover, dissociation of ClpP into heptamers was also observed upon the addition of irreversible active-site inhibitors.^[17] These findings suggest that disproportionation of ClpP tetradecamers and the formation of transient complexes might be a conserved feature of this class of proteases.

While the exact biological role of LmClpP1/2 is elusive, we noticed that an elevated catalytic rate, as observed with the heterocomplex in association with ClpX, may aid the rapid removal of unfolded proteins under stress conditions such as host-cell invasion. This is supported by real-time PCR studies, which show a 7-fold up-regulation of LmClpP1 and LmClpP2 transcript levels upon heat stress (Figure S14). Furthermore, customized specificities towards defined peptidic substrates can be predicted from the crystallographic results^[9] as a result of pronounced differences in the shapes of the corresponding binding pockets. In particular, the S1 site of LmClpP1 exhibits a restricted architecture that is significant for the recognition of smaller substrates. This architecture increases affinity and extends the duration of binding, and it may thereby compensate for the reduced catalytic activity of the Ser-His-Asn center. Future work should thus focus on the design of selective LmClpP1 and LmClpP2 inhibitors for the treatment of *L. monocytogenes* infections, which now can be addressed on the basis of structure-activity relationships.

Note: While this paper was under review, Sauer and colleagues published the crystal structure of the *M. tuberculosis* ClpP1/2 heterocomplex in association with two ligands: an acyldepsipeptide (ADEP) and an agonist peptide.^[18] Unlike LmClpP1/2, MtClpP1/2 heterocomplex assembly requires the aid of these peptides, which synergistically activate proteolysis. The structures of the two enzyme complexes thus provide complementary mechanistic insights.

Received: September 21, 2014

Revised: November 10, 2014

Published online: January 28, 2015

Keywords: ClpP · enzyme catalysis · heterocomplexes · protein structures · proteolysis

- [1] a) T. A. Baker, R. T. Sauer, *Biochim. Biophys. Acta Mol. Cell Res.* **2012**, 1823, 15–28; b) Y. Katayama-Fujimura, S. Gottesman, M. R. Maurizi, *J. Biol. Chem.* **1987**, 262, 4477–4485; c) D. Frees, S. N. Qazi, P. J. Hill, H. Ingmer, *Mol. Microbiol.* **2003**, 48, 1565–1578.
- [2] a) M. R. Maurizi, W. P. Clark, Y. Katayama, S. Rudikoff, J. Pumphrey, B. Bowers, S. Gottesman, *J. Biol. Chem.* **1990**, 265, 12536–12545; b) J. Wang, J. A. Hartling, J. M. Flanagan, *Cell* **1997**, 91, 447–456.
- [3] a) M. C. Bewley, V. Graziano, K. Griffin, J. M. Flanagan, *J. Struct. Biol.* **2009**, 165, 118–125; b) A. Gribun, M. S. Kimber, R. Ching, R. Sprangers, K. M. Fiebig, W. A. Houry, *J. Biol. Chem.* **2005**, 280, 16185–16196.
- [4] a) M. W. Thompson, M. R. Maurizi, *J. Biol. Chem.* **1994**, 269, 18201–18208; b) A. Battesti, S. Gottesman, *Curr. Opin. Microbiol.* **2013**, 16, 140–147; c) E. U. Weber-Ban, B. G. Reid, A. D. Miranker, A. L. Horwich, *Nature* **1999**, 401, 90–93.
- [5] S. Gottesman, E. Roche, Y. Zhou, R. T. Sauer, *Genes Dev.* **1998**, 12, 1338–1347.
- [6] O. Gaillot, E. Pellegrini, S. Bregenholt, S. Nair, P. Berche, *Mol. Microbiol.* **2000**, 35, 1286–1294.
- [7] a) E. Zeiler, N. Braun, T. Bottcher, A. Kastenmuller, S. Weinkauff, S. A. Sieber, *Angew. Chem. Int. Ed.* **2011**, 50, 11001–11004; *Angew. Chem.* **2011**, 123, 11193–11197; b) T. Akopian, O. Kandror, R. M. Raju, M. Unnikrishnan, E. J. Rubin, A. L. Goldberg, *EMBO J.* **2012**, 31, 1529–1541; c) R. M. Raju, M. Unnikrishnan, D. H. Rubin, V. Krishnamoorthy, O. Kandror, T. N. Akopian, A. L. Goldberg, E. J. Rubin, *PLoS Pathog.* **2012**, 8, e1002511.
- [8] J. A. Vazquez-Boland, M. Kuhn, P. Berche, T. Chakraborty, G. Dominguez-Bernal, W. Goebel, B. Gonzalez-Zorn, J. Wehland, J. Kreft, *Clin. Microbiol. Rev.* **2001**, 14, 584–640.
- [9] E. Zeiler, A. List, F. Alte, M. Gersch, R. Wachtel, M. Poreba, M. Drag, M. Groll, S. A. Sieber, *Proc. Natl. Acad. Sci. USA* **2013**, 110, 11302–11307.
- [10] Y. I. Kim, R. E. Burton, B. M. Burton, R. T. Sauer, T. A. Baker, *Mol. Cell* **2000**, 5, 639–648.
- [11] K. R. Schmitz, R. T. Sauer, *Mol. Microbiol.* **2014**, 93, 617–628.
- [12] M. C. Bewley, V. Graziano, K. Griffin, J. M. Flanagan, *J. Struct. Biol.* **2006**, 153, 113–128.
- [13] M. Gersch, A. List, M. Groll, S. A. Sieber, *J. Biol. Chem.* **2012**, 287, 9484–9494.
- [14] K. Liu, A. Ologbenla, W. A. Houry, *Crit. Rev. Biochem. Mol. Biol.* **2014**, 1–13.
- [15] A. Szyk, M. R. Maurizi, *J. Struct. Biol.* **2006**, 156, 165–174.
- [16] a) S. R. Geiger, T. Bottcher, S. A. Sieber, P. Cramer, *Angew. Chem. Int. Ed.* **2011**, 50, 5749–5752; *Angew. Chem.* **2011**, 123, 5867–5871; b) J. Zhang, F. Ye, L. Lan, H. Jiang, C. Luo, C. G. Yang, *J. Biol. Chem.* **2011**, 286, 37590–37601.
- [17] M. Gersch, R. Kolb, F. Alte, M. Groll, S. A. Sieber, *J. Am. Chem. Soc.* **2014**, 136, 1360–1366.
- [18] K. R. Schmitz, D. W. Carney, J. K. Sello, R. T. Sauer, *Proc. Natl. Acad. Sci. USA* **2014**, 111, E4587–4595.